THE JOURNAL OF PHYSICAL CHEMISTRY Letters

pubs.acs.org/JPCL

Optical Trapping of Quantum Dots Based on Gap-Mode-Excitation of Localized Surface Plasmon

Yasuyuki Tsuboi,*,† Tatsuya Shoji,† Noboru Kitamura,*,† Mai Takase,† Kei Murakoshi,† Yoshihiko Mizumoto,‡ and Hajime Ishihara‡

†Division of Chemistry, Graduate School of Science, Hokkaido University, Sapporo 060-0810, Japan, and ‡Department of Physics and Electronics, Osaka Prefecture University, Gakuencho 1-1, Nakaku 599-8531, Sakai, Osaka, Japan.

ABSTRACT One of the recent hot topics in the fields of plasmonics and related nanophotonics is optical trapping of nano/microparticles based on surface plasmon. Experimental demonstration of such trapping by gap-mode plasmon has hitherto been limited so far to a few reports in which submicrometer polymer beads were trapped with intense irradiation at MW/cm^2, satisfying an energetic condition of $U > kT$. (U is the potential energy of the trap and kT is an averaged thermal background energy.) We demonstrate plasmon-based optical trapping of a luminescent quantum dot (Q dot, diameter ≥10 nm) with a very weak irradiation (0.5−10 kW/cm^2). The most important discovery is that the Q dot trapping was clearly observed through luminescence detection even under an energetic condition of $U < kT$, on the basis of which we propose a novel concept that is peculiar to plasmon-based trapping at a nanogap.

SECTION Nanoparticles and Nanostructures

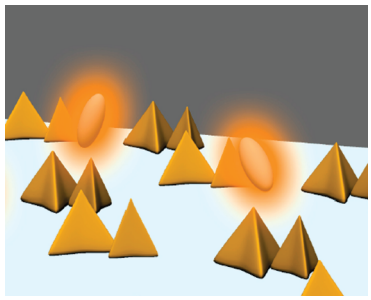

Plasmonics involves a wealth of novel promising scientific applications, and one such challenging application is the trapping of nanomaterial in a nanospace by an enhanced optical force.[1] It is well known that photons can exert a mechanical force on a nanoparticle, and this has been extensively used in creating optical tweezers.[2] Optical trapping based on surface plasmon can potentially overcome the disadvantages of the conventional optical trapping technique; these disadvantages are that (i) the conventional technique requires intense focused laser light to manipulate a small nanoparticle[3,4] and (ii) the spatial resolution in trapping is ordinarily limited to more than several hundreds of nanometers because of the diffraction limit of the incident light.

Optical trapping of nanoparticles based on surface plasmon has been theoretically predicted and analyzed by several groups in the past decade.[5] In particular, in 2006, Quidant et al. reported on a theoretical treatment of and first demonstrated an experiment on a plasmon-based radiation force exerted on a single polystyrene bead.[6] Moreover, they succeeded in parallel and selective trapping of polystyrene beads (diameter (d) ≈ 5 μm) in a patterned plasmonic landscape.[7] As has been predicted theoretically and verified experimentally, the electromagnetic field of incident light should be strongly localized and considerably enhanced at the nanojunction or nanogap between adjacent metallic nanoparticles. However, experimental demonstration of such plasmon-based optical trapping utilizing the gap-mode excitation has hitherto been limited to only few works. Grigorenko et al. recently demonstrated the optical trapping of polystyrene beads (d = 0.2−6 μm) at such nanogaps using gold nanodots.[8] In this case, the gap width was somewhat large (width was ranging from 20−200 nm) and hence focusing of the intense laser beam (irradiation power P = 150 mW, corresponding to an intensity I > 0.15 MW/cm^2) was needed for stable trapping. In 2009, Righini and Quidant et al. succeeded in the stable optical trapping of polystyrene beads (d = 200 nm) under much less intense irradiation conditions (I ≈ kW/cm^2) using a gold nanogap antenna (gap width ∼30 nm).[9]

These studies indicate that such metallic nanostructures (nanogap, nanojunction, nanoantenna, nanobowtie, etc.) can function as novel small light sources in the nanospace. The important factor in such plasmon-based optical trapping is the interaction energy U between the nanoparticle and the plasmon-enhanced electromagnetic field. For stable trapping, the potential energy U is required to satisfy the simple relation $U > kT$, where k is the Boltzmann constant and T is temperature, by analogy to conventional optical trapping. Because the use of a nanogap as a novel light source provides a specific electromagnetic field that obviously differs from that of conventional propagating light waves, there are various factors we need to consider and that need to be examined for the establishment of plasmon-based optical trapping.

Here we demonstrate the plasmon-based optical trapping of a very small semiconductor quantum dot (Q dot, d ≈ 10 nm) with considerably weak light irradiation. Because a theoretical analysis was recently performed, Q dots are intriguing as well as challenging targets for plasmon-based optical

Received Date: May 19, 2010
Accepted Date: July 6, 2010

DOI: 10.1021/jz100659x | J. Phys. Chem. Lett. 2010, 1, 2327–2333

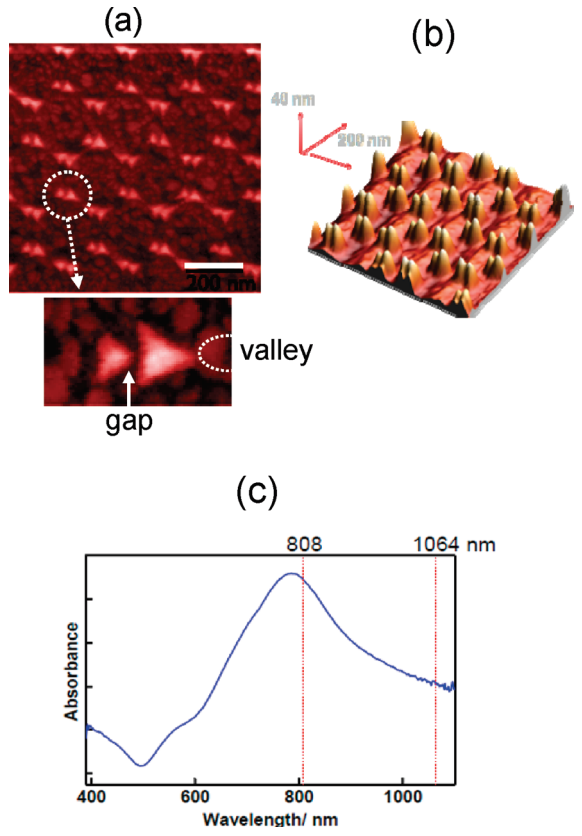

Figure 1. Surface morphology and optical property of the AR-NSL gold substrate used in the present study. (a) Scanning electron micrograph. Scale: bar = 200 nm. (b) AFM image in 3D. (c) Optical absorption spectrum.

trapping[10] because the realization of $U > kT$ is generally difficult for nonmetallic nano-objects. However, it is interesting that peculiar kinetic motions of Q dots induced by plasmon excitations are clearly monitored even under $U < kT$ in our demonstration, where a luminescence property of a Q dot enables us to get insight into what is going on at the nanospace by analyzing the photoluminescence behavior. This demonstration raises intriguing issues for the comprehensive understanding of the plasmon-based trapping at a nanogap and would enhance the concept of optical trapping using a novel light source at a metallic nanogap.

We fabricated gold nanodimer arrays on a plasmonic glass substrate using the technique of angle-resolved nanosphere lithography (AR-NSL), the details of which have already been described.[11,12] Figure 1a displays a scanning electron microscope (SEM) image of the NSL substrate. In each dimer, adjacent triangular nanoblocks are separated by a nanogap (Figure 1a, magnified image). The detailed 3D structure of the NSL substrate morphology was revealed using atomic force microscopy (AFM), as shown in Figure 1b. The height of each dimer and the distance between adjacent dimers were evaluated to be 30 and 140 nm, respectively. That is, the NSL substrate has two types of nanotrapping gap site. One site is a narrow nanogap (width >10 nm) at the center of each dimer, whereas the other corresponds to the relatively wider "valley" (width <150 nm) located between adjacent dimers. (See Figure 1a.) The optical absorption spectrum of the NSL substrate is shown in Figure 1c. The resonant surface plasmon band of individual gold nanoparticles almost disappears at around 500−600 nm; instead, a broad absorption band is realized in a wider near-infrared (NIR) region going above 1 μm. This broad NIR band can be ascribed to plasmonic gap-mode absorption. That is, in exciting the gap-mode transitions with NIR light irradiation, the electromagnetic field of the incident light becomes remarkably enhanced around the trapping sites.

As a target material, we singled out a fluorescent quantum dot (Q dot): a CdSe/ZnS core−shell nanoparticle, which has dimensions of 11 nm (long axis) and 5 nm in diameter (short axis). The core CdSe is coated with ZnS (layer thickness, 0.2 to 0.7 nm) and a polymer layer (thickness < 1 nm). The main experiments were performed in the following manner. The 488 nm laser light was irradiated during the observation period (always on). Simultaneously, 808 nm laser light was irradiated in a repetitive on-and-off mode, and photoluminescence from the focal point was monitored continuously under a confocal optical microscope.[3,4] (See the Materials and Methods section.)

Before describing the main results, we briefly note some features of the Q dots used here (for details, see Supporting Information). First, the Q dots are thermally tough. The photoluminescence intensity did not decrease very much even when the solution temperature was raised close to boiling point. Second, the photoluminescence of the Q dots did not undergo plasmonic photoluminescence enhancement when the Q dots were adsorbed on or located close to the NSL gold nanoblocks. Instead of photoluminescence enhancement we observed photoluminescence quenching by the NSL gold nanoblocks.

In the presence of the NSL gold substrate, we discovered some quite intriguing photoluminescence behavior of the Q dots. The photoluminescence intensity responds sensitively to the switching on and off of the 808 nm laser light. Representative results of the photoluminescence spectra and time traces of the luminescent intensity are displayed in Figure 2 for the case without poly(ethylene glycol) (PEG). (See the Materials and Methods section.) Without 808 nm laser irradiation, the emission was observed with a peak at 610 nm, and this can safely be ascribed to Q dot photoluminescence induced by the 488 nm light irradiation. Just after switching on the 808 nm laser irradiation, the photoluminescence intensity suddenly dropped and was almost completely quenched. Then, upon switching off the 808 nm laser, the photoluminescence rapidly recovered to the original intensity. This cycle can be repeated with good reproducibility by switching the irradiation on and off. Furthermore, we found that this interesting behavior took place beyond a certain threshold value with respect to the light intensity, $I_{th} \approx 3-5$ kW/cm^2 at 808 nm.

These results clearly show that the photoluminescence of individual Q dots is promptly quenched by the excitation of a plasmonic gap-mode transition of the NSL gold nanoblocks. Because the temperature rise upon NIR irradiation is considerably small ($\Delta T \approx 0.1$ K at 1 kW/cm^2, see Supporting Information) around the gold nanoblocks and the Q dot photoluminescence intensity is hardly affected by raising the temperature, the quenching behavior can be ascribed to

DOI: 10.1021/jz100659x | J. Phys. Chem. Lett. 2010, 1, 2327–2333

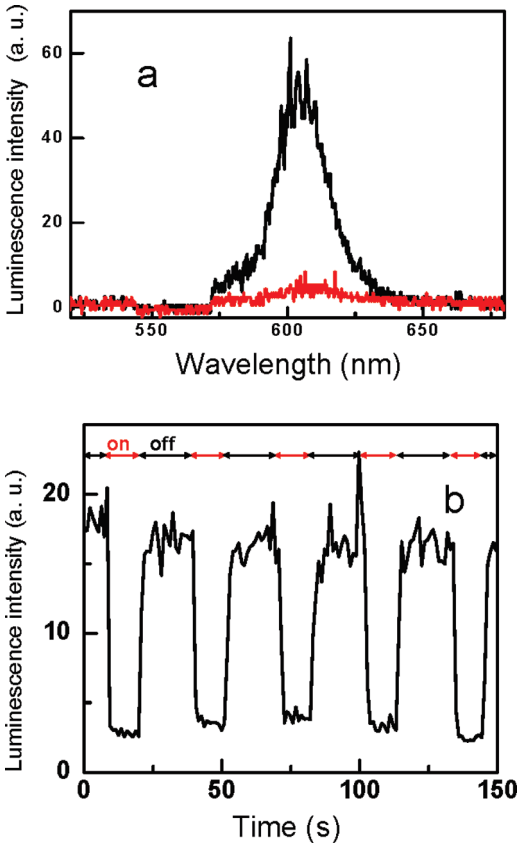

Figure 2. Optical trapping behavior of Q dots in the present system (8×10^{-9} mol/L aqueous solution in the presence of AR-NSL gold nanostructure). (a) Photoluminescence spectra. Black line: before irradiation at 808 nm. Red line: during irradiation at 808 nm. (b) Modulation (temporal profile) of the photoluminescence intensity in line with the plasmonic excitation by repeatedly switching the 808 nm irradiation (I = 10 kW/cm^2) on and off. Data points were collected every 1.0 s step in 3.8 ms intervals.

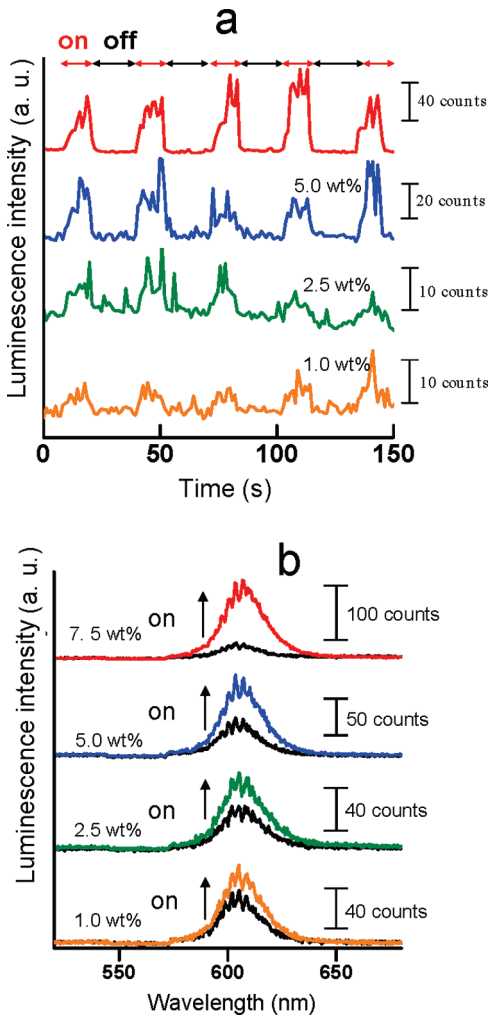

Figure 3. Optical trapping behavior of Q dots in the presence of poly(ethylene glycol) (PEG). The scale of the luminescence intensity (counts in the CCD camera) and the PEG concentration are given. (a) Modulation (temporal profile) of the photoluminescence intensity in line with the plasmonic excitation by repeatedly switching the 808 nm irradiation (I = 1.0 kW/cm^2) on and off. Data points were collected every 1.0 s step in 3.8 ms intervals. (b) Photoluminescence spectra. Spectra before irradiation at 808 nm are plotted in black, whereas those measured during irradiation at 808 nm are plotted in color.

an effect of localized surface plasmon, and this is discussed in detail later.

As described in the Materials and Methods section, the Q dots used here undergo assembly in the presence of PEG because of the effect of volume exclusion. The repetitive on-and-off NIR irradiation experiments were also carried out for sample solutions containing PEG, and representative results are displayed in Figure 3 for various PEG concentration (1.0, 2.5, 5.0, and 7.5 wt %). Also, in these cases, the Q dot photoluminescence intensity responded to the NIR irradiation. What is interesting here is that the photoluminescence intensity switches in the opposite direction compared with the case in the absence of PEG. That is, the photoluminescence of the Q dot clusters, rather than decreasing, increases markedly on exposure to the 808 nm irradiation. After the irradiation is switched off, the photoluminescence again decreases to its original intensity, and this cycle can be repeated with good reproducibility by switching the NIR irradiation on and off.

This behavior was observed for sample solutions irrespective of the PEG concentration, and the photoluminescence intensity became higher with increasing concentration. Furthermore, we discovered the important fact that there is a threshold value (I_{th}) of the irradiation intensity for this switching phenomenon. We estimated I_{th} to be ~0.5 kW/cm^2 (P_{th} = 90 μW) for the present sample solutions. Here we define the photoluminescence enhancement factor F_e; $F_e = I_{on}/I_{off}$ where I_{on} and I_{off} are the photoluminescence intensities in the presence and absence of NIR irradiation, respectively. In Figure 4, the enhancement factor F_e is plotted as a function of PEG concentration with varying (I = 1.0−4.0 kW/cm^2). As seen in the Figure, F_e increases from 1.5 to >10 with increasing PEG concentration from 1.0 to 7.5 wt %, obviously indicating that larger Q dot clusters induce photoluminescence enhancement. It should be pointed out here that the enhancement factor F hardly depends on the laser intensity, I.

Such photoluminescence behavior can also be readily visualized by microscopic imaging, as shown in Figure 5.

DOI: 10.1021/jz100659x | J. Phys. Chem. Lett. 2010, 1, 2327–2333

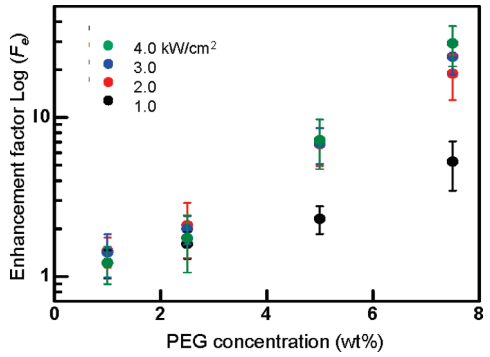

Figure 4. Enhancement factor F_e ($F_e = I_{on}/I_{off}$) as a function of PEG concentration at different 808 nm laser intensities.

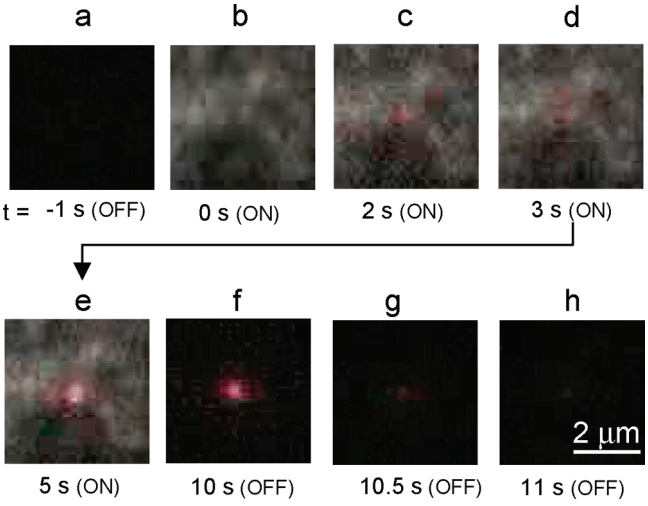

Figure 5. Optical micrographs of the temporal behavior of Q dot trapping by 808 nm irradiation. The PEG concentration was 5.0 wt %, and the irradiation intensity was 3.0 kW/cm^2. ON and OFF refers to the condition of the 808 nm laser irradiation. During observation, the 488 nm laser was always focused at the center area in the images. (a) Observation time $t = -1$ s means 1s before switching on the 808 nm irradiation. (b) $t = 0$ s corresponds to the time at which the 808 nm laser is switched ON. (f) $t = 10$s corresponds to the time at which the 808 nm laser is switched OFF. The scale is given in (h).

(A video image is available in the Supporting Information.) Before the 808 nm irradiation, photoluminescence should be weakly induced by 488 nm excitation around the center area of the picture frame (but it is too weak to be seen in Figure 5a). On starting the 808 nm irradiation ($t = 0$ s), the irradiation spot is seen as a slightly bright area in Figure 5b. Approximately 1 to 2 s later, the onset of Q dot photoluminescence is manifested (Figure 5c) and becomes brighter with time (Figure 5d,e). After the 808 nm irradiation is terminated, the Q dot photoluminescence still remains (Figure 5f), but it decays gradually with time (Figure 5g,h). Therefore, the trapping behavior can be readily visualized by monitoring the photoluminescence. We clearly detected short time intervals both between starting the irradiation and the rise in photoluminescence and between stopping the irradiation and photoluminescence decay.

What we have revealed experimentally can be summarized as follows (Other features are given in the Supporting Information). (i) In the absence of PEG, Q dot photoluminescence is clearly and completely quenched by NIR irradiation beyond a certain threshold ($I_{th} \approx 5$ kW/cm^2). (ii) In the presence of PEG, Q dot photoluminescence is clearly enhanced by NIR irradiation beyond a certain threshold ($I_{th} \approx 0.5$ kW/cm^2). (iii) The enhancement factor F_e increases with increasing size of the Q dot cluster, whereas it scarcely depends upon laser intensity.

For result i, photoluminescence quenching, one possible explanation for this is optical trapping of Q dots at the nanogaps of the NSL gold structure because we have confirmed that it is clearly not due to thermal quenching and that the photoluminescence was quenched in the vicinity of the NSL gold nanoblocks. Presumably, Q dots that move around the NSL gold nanoblocks by Brownian motion would be optically trapped at the nanogaps, where localized surface plasmons are excited by NIR irradiation.

For result ii, a plausible mechanism for the photoluminescence enhancement is two-photon excitation of Q dots by NIR light at the nanogaps based on an enhancement effect of the electromagnetic field of the incident NIR light by localized surface plasmon, as we and Ueno et al. recently demonstrated.[13,14] However, this effect can be readily excluded because the Q dot photoluminescence was not observed when the 488 nm irradiation was off whether the NIR irradiation was on or off. Namely, the Q dot photoluminescence was simply induced by one-photon absorption at 488 nm.

By integrating these results, we may conclude that optical trapping at nanogaps/nanovalleys induces photoluminescence quenching and enhancement. As previously described, the Q dots used here form clusters in the presence of PEG, and the size of the cluster increases with increasing PEG concentration. In the framework of a simple theory of optical trapping, the trapping potential energy should be proportional to the size (volume, r^3 where r is radius) of the particle to be trapped. Therefore, it is natural to expect that the addition of PEG to the sample solutions promotes optical trapping of Q dots, resulting in photoluminescence enhancement. Indeed, the deduction is well consistent with the experimental facts that the value of I_{th} in the absence of PEG is significantly higher than that in the presence of PEG and that the enhancement factor F_e increases with increasing PEG concentration (iii). As noted already, we can observe approximately 6−10 nanogaps and nanovalleys within the experimental field of view, whereas, on average, there should be 1 to 2 Q dots. The results shown in Figure 4, where F_e is $<10-20$ at most, do not contradict this. (Each trapping site would trap 1 to 2 Q dot cluster/clusters.) Also, in this case, photoluminescence of Q dots at the most outer shell in a cluster would be quenched. However, Q dots located inside the cluster would still emit photoluminescence, resulting in the luminescence enhancement. In addition, PEG plays a role as a spacer, preventing luminescence quenching that efficiently takes place when a distance between fluorophore and a Au nanoparticle <5 nm.[15]

To clarify these observations quantitatively, we performed a theoretical calculation for the spatial distribution of the enhanced electric field and trapping potential created by

DOI: 10.1021/jz100659x | J. Phys. Chem. Lett. 2010, 1, 2327–2333

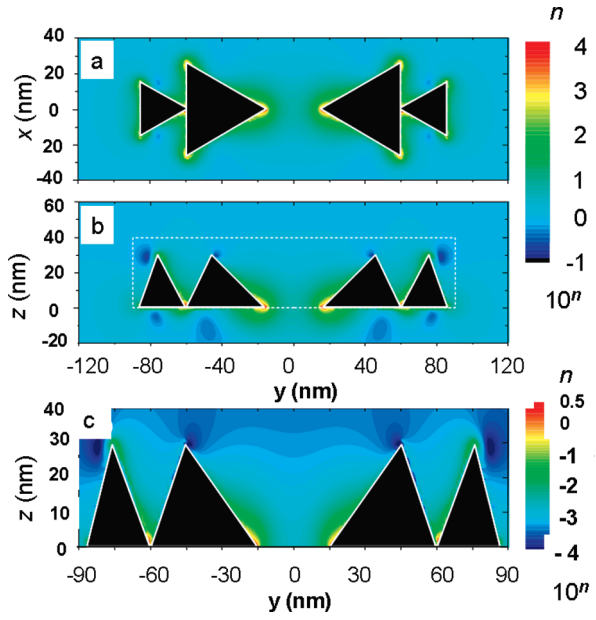

Figure 6. Theoretical calculation using Maxwell equation based on discrete dipole approximation (DDA). (a) Top view of gold nanodimer used in this calculation and enhancement factor of the electric field intensity as function of x and y at $z = 0$. The color scale is on a logarithmic scale. (b) Side view of gold nanodimer used in this calculation and enhancement factor of the electric field intensity as function of z and y at $x = 0$. The color scale is on a logarithmic scale. (c) Spatial distribution of trapping potential (U) at the nanovalley (marked with white dotted-line box in part b) when $I = 1.0$ kW/cm^2 and radius of Q dot particle is 15 nm. The color scale gives the potential energy normalized with kT on a logarithmic scale.

surface plasmon localized around the gold nanodimer by solving the discretized integral form of the Maxwell equations based on the discrete dipole approximation (DDA).[16] In this calculation, we divide the space, including the metal blocks, into small cubic cells, where microscopic quantities such as the electric field and polarization in the each cell are averaged over the volume integral in the analytical evaluation of the self-interaction. The integral equation is given by

$$\mathbf{E}_i = \mathbf{E}^0{}_i + \sum_{j=1}^{N} \mathbf{G}^{\mathrm{f}}{}_{i,j}\mathbf{P}_j V_j \qquad (1)$$

where $\mathbf{P}_j = \chi_j \mathbf{E}_j$ is satisfied in each cell. χ_j is the optical susceptibility, i is the number of the cell at the observation position ($i = 1, ..., N$), j is the number at the source position ($j = 1, ..., N$), $\mathbf{E}_i$ is the total response field, $\mathbf{E}_i^0$ is the incident field, $\mathbf{G}_{i,j}^{\mathrm{f}}$ is the free space Green function with both the transverse and longitudinal electromagnetic components, and V_j is the volume of the jth cell. The metal blocks are assumed to have a Drude-type dielectric function with the parameters of gold.[17,18]

As a representative example, the following experimental parameters were used: $I = 1.0$ kW/cm^2, the radius of the Q dot particle was 15 nm, and the NSL gold nanodimer pair used had the 3D figure illustrated in Figure 6a,b (top and side views, respectively). Figure 6a,b shows a profile of the electric field intensity as a function of x and y at $z = 0$ and a function of z and y at $x = 0$, respectively. (The coordinates are indicated in the Figures.) Here the y axis is a coordinate along a cross section of the gold nanodimer in the long axis. The electric field is strongly enhanced at the valley position and in the gap between the folded blocks. We then evaluated the trapping potential U along the z axis from the calculated electric field by using the standard formula based on the dipole approximation,[19] taking the Lorents force and stress tensor into account.

Figure 6c shows the zy map of $\log(U/kT)$ at $x = 0$ in the region indicated by the dotted line rectangle in Figure 6b. Although this Figure shows regions of $U > kT$ near the edges and gaps of the metal blocks, it is estimated that in reality $U < kT$ because the spatial extension of the particles is much larger than that of the area where $U > kT$. It is noteworthy here that threshold laser power (I_{th}) required for trapping is lower than those in preceding works.[7,8] This is partially due to a contrast in refractive index (n). In the present case, n of CdSe and water are 2.4 and 1.3, respectively, which is much higher contrast as compared with the preceding works.

From the above estimation, we can say that the observed kinetic behavior of the nanoparticles is induced by traps shallower than kT. This seems to indicate that for the observed peculiar kinetic motion of the nanoparticles induced by local plasmon, $U > kT$ is not an indispensable requirement both for single Q dots and Q dot clusters. Indeed, the light intensity used here is 1−10 kW/cm^2, which is one or two orders of magnitude smaller than that used in a quite recent study for trapping 10 nm sized gold nanoparticles.[20] Several mechanisms should be taken into account to elucidate the behavior, and here we propose one possible candidate for the explanation. In preceding trapping studies using metallic nanogaps, one characteristic feature described was a mutual dimensional relationship between the nanoparticle and the nanogap. Namely, in those studies, the size of the nanoparticles to be trapped was comparable to or significantly larger than the width of the nanogap,[8,9,19] meaning that the nanoparticle never got into the gap but was just adsorbed near the gap. In contrast, this dimensional relationship is inverted in our present study, which would enable a Q dot or a Q dot cluster to get into the nanogap or nanovalley. Q dots or Q dot clusters move by Brownian motion in solution (the diffusion length is ca. 5−10 μm per a second), and when they get close to a gold nanostructure where surface plasmons are excited, they would be attracted toward the nanogap or nano valley. Once trapped at the gap or valley, they feel an intense electromagnetic field from the gold nanoblocks surrounding them. In addition, the gold nanoblocks hinder their escape. Consequently, the average trapping time of a single Q dot in a nanogap or a Q dot cluster in a nanovalley becomes longer, and the motional behavior of the Q dots and Q dot clusters would be as if they were bound. Furthermore, we should point out an additional force in the nanospace that would act in favor of the trapping. One powerful candidate is the van der Waals force. To elucidate the present trapping behavior, a discussion in terms not only of electromagnetic physics (examined here) but also of another physical insight is necessary. The present results suggest that the hydrodynamics or fluid mechanic should be taken into account.

The present phenomenon can presumably be categorized as optical bondage in a nanogap, whose whole picture would

DOI: 10.1021/jz100659x | J. Phys. Chem. Lett. 2010, 1, 2327–2333

be clarified by the systematic and detailed dynamics-based analysis of nano-objects near a metallic nanogap. To elucidate such picture quantitatively is a next issue that is proposed here and is currently progress. Therefore, the present study will open the possibility of enhancing the degrees of freedom to manipulate nano-objects for next-generation nanoscience and technologies.

MATERIALS ANDS METHODS

The Q dots were supplied from Invitrogen (Q dot 605). They can be stably and homogeneously dispersed in water (8×10^{-9} mol/L). The optical spectra and a TEM image of the quantum dots are given in the Supporting Information. In some cases, PEG (molecular weight $\approx$ 6000) was added to the aqueous Q dot solution to induce assembly of the Q dots by the volume exclusion effect in solution. We controlled the size of the Q dot cluster (assembly) by varying the concentration of PEG in the solution: the average diameter (d) of the Q dot assembly at different PEG concentrations was d = 11 (PEG concentration, 0 wt %), 30 (1.0 wt %), 50 (2.5 wt %), 70−80 (5.0 wt %), and >70 nm (7.5 wt %) These sample solutions were used as liquid membranes sandwiched between the NSL substrate and a coverslip.

A confocal spectroscopic microscope[3,4] was used to explore optical trapping of the Q dot. (For details, see the Supporting Information.) Continuous wave (CW) Ar^+ laser light (488 nm, irradiation power $P \approx 20$ μW) used for Q dot photoluminescence excitation was introduced into the microscope. A coaxial CW-NIR diode laser beam (808 nm) or CW YAG laser beam (1064 nm) was also introduced into the microscope for excitation of the plasmonic band gap of the NIR substrate. Note that the Q dots are completely transparent to NIR light (see the absorption spectrum given in the Supporting Information) and that the intensity at the focal point (at the sample position) is weak (P < 1 mW, irradiation intensity I < 10 kW/cm^2, see later). In this confocal arrangement, the observation area was x, y < 500 nm (laterally) and $z \approx 2$ μm (in depth). In this observation volume (3×10^{-13} cm^3), there should be about 6 to 10 gold dimers and 1 to 2 quantum dots according to a simple calculation. The main experiment was performed in the following manner. The 488 nm laser light was irradiated during the observation period (always on). Simultaneously, 808 nm laser light was irradiated in a repetitive on-and-off mode, and photoluminescence from the focal point was monitored continuously.

SUPPORTING INFORMATION AVAILABLE Detailed experimental set up, optical and thermal properties of the Q dot, conventional optical trapping the Q dot, other features of the present plasmon-based trapping, and a video image. This material is available free of charge via the Internet at http://pubs.acs.org.

AUTHOR INFORMATION

Corresponding Author:

*To whom correspondence should be addressed. E-mail: twoboys@sci.hokudai.ac.jp (Y.T.), kitamura@sci.hokudai.ac.jp (N.K.).

ACKNOWLEDGMENT We are grateful to Dr. H. Shimomoto and Prof. S. Aoshima at Osaka University for measurement of the light scattering of Q dots. We also thank Dr. Ichihara (Otsuka Electric) for the measurements of Q dot diameters. We appreciate the work of Dr. K. Okazaki and Prof. Tsukasa Torimoto (Nagoya University) for the TEM measurements. This work was partially supported by a Grant-in-Aid for Scientific Research from the Ministry of Education, Culture, Sports, Science and Technology of Japan for the Priority Area "Strong Photons-Molecules Coupling Fields (470)" (no. 19049004), no. 20550002, and the Global COE Program (project no. B01: Catalysis as the Basis for Innovation in Materials Science).

REFERENCES

(1) Hallock, A. J.; Redmond, P. L.; Brus, L. E. Optical Force between Metallic Particles. *Proc. Natl. Acad. Sci. U.S.A.* **2005,** *102*, 1280–1284.

(2) Ashkin, A.; Dziedzic, J. M.; Yamane, T. Optical Trapping and Manipulation of Single Cells Using Infrared Laser Beams. *Nature* **1987,** *330*, 769–771.

(3) Tsuboi, Y.; Nishino, M.; Sasaki, T.; Kitamura, N. Poly(*N*-isopropylacrylamide) Microparticles Produced by Radiation Pressure of a Focused Laser Beam: A Structural Analysis by Confocal Raman Microspectroscopy Combined with a Laser-Trapping Technique. *J. Phys. Chem. B* **2005,** *109*, 7033–7039.

(4) Tsuboi, Y.; Shoji, T.; Kitamura, N. Optical Trapping of Amino Acids in Aqueous Solutions. *J. Phys. Chem. C* **2010,** *114*, 5589–5593.

(5) Quidant, R.; Girard, C. Surface-Plasmon-Based Optical Manipulation. *Laser Photon. Rev.* **2008,** *2*, 47–57.

(6) Volpe, G.; Quidant, R.; Badenes, G.; Petrov, D. Surface plasmon radiation Forces. *Phys. Rev. Lett.* **2006,** *96*, 238101.

(7) Righini, M.; Zelenina, A. S.; Girard, C.; Quidant, R. Parallel and Selective Trapping in a Patterned Plasmonic Landscape. *Nature Phys.* **2007,** *3*, 477–480.

(8) Grigorenko, A. N.; Roberts, N. W.; Dickinson, M. R.; Zhang, Y. Nanometric Optical Tweezers Based on Nanostructured Substrates. *Nature Photon.* **2008,** *2*, 365–370.

(9) Righini, M.; Ghenuche, P.; Cherukulappurath, S.; Myroshnychenko, V.; García de Abajo, F. J.; Quidant, R. Nano-Optical Trapping of Rayleigh Particles and *Escherichia coli* Bacteria with Resonant Optical Antennas. *Nano Lett.* **2009,** *9*, 3387–3391.

(10) Dineen, C.; Reichelt, M.; Koch, S. W.; Moloney, J. V. Optical Trapping of Quantum Dots in a Metallic Nanotrap. *J. Opt. A: Pure Appl. Opt.* **2009,** *11*, 114004.

(11) Haynes, C. L.; McFarland, A. D.; Smith, M. T.; Hulteen, J. C.; Van Duyne, R. P. Angle-Resolved Nanosphere Lithography: Manipulation of Nanoparticle Size, Shape, And Interparticle Spacing. *J. Phys. Chem. B* **2002,** *106*, 1898–1902.

(12) Ikeda, K.; Takase, M.; Sawai, Y.; Nabika, H.; Murakoshi, K.; Uosaki, K. Hyper-Raman Scattering Enhanced by Anisotropic Dimmer Plasmons on Artificial Nanostructures. *J. Chem. Phys.* **2007,** *127*, 111103–01 −111103−04.

(13) Tsuboi, Y.; Shimizu, R.; Shoji, T.; Kitamura, N. Near-Infrared Continuous-Wave Light Driving a Two-Photon Photochromic Reaction with the Assistance of Localized Surface Plasmon. *J. Am. Chem. Soc.* **2009,** *131*, 12623–12627.

(14) Ueno, K.; Juodkazis, S.; Shibuya, T.; Yokota, Y.; Mizeikis, V.; Sasaki, K.; Misawa, H. Nanoparticle Plasmon-Assisted Two-Photon Polymerization Induced by Incoherent Excitation Source. *J. Am. Chem. Soc.* **2008,** *130*, 6928–6929.

(15) Anger, P.; Bharadwaj, P.; Novotny, L. Enhancement and Quenching of Single-Molecule Fluorescence. *Phys. Rev. Lett.* **2006,** *96*, 113002−1 −113002−4.

(16) Purcell, E. M.; Pennypacker, C. R. Scattering and Absorption of Light by Nonspherical Dielectric Grains. *Astrophys. J.* **1973,** *186*, 705–714.

(17) Johnson, P. B.; Christy, R. W. Optical Constants of the Noble Metals. *Phys. Rev. B* **1972,** *6*, 4370–4379.
(18) Antoine, R.; Brevet, P. F.; Girault, H. H.; Bethell, D.; Schiffrin, D. J. Surface Plasmon Enhanced Non-Linear Optical Response of Gold Nanoparticles at the Air/Toluene Interface. *Chem. Commun.* **1997,** 1901–1902.
(19) Ashkin, A.; Dziedzic, J. M.; Bjorkhohn, J. E.; Chu, S. Observation of a Single-Beam Gradient Force Optical Trap for Dielectric Particles. *Opt. Lett.* **1986,** *11*, 288–290.
(20) Zhang, W.; Huang, L.; Santschi, C.; Martin, O. J. F. Trapping and Sensing 10 nm Metal Nanoparticles Using Plasmonic Dipole Antennas. *Nano Lett.* **2010,** *10*, 1006–1011.

DOI: 10.1021/jz100659x | *J. Phys. Chem. Lett.* **2010,** *1,* 2327–2333